



Luminescence Properties of $\text{Ba}_3\text{Si}_6\text{O}_{12}\text{N}_2:\text{Eu}^{2+}$ Green Phosphor

Van Duong Luong^a, Dinh Phuong Doan^a, Hong-Ro Lee^{b*}

^aInstitute of Materials Science, Vietnam Academy of Science and Technology, 18 Hoang Quoc Viet Road, Cau Giay District, Hanoi, Vietnam

^bDepartment of Advanced Materials Engineering, Chungnam National University, Daejeon 305-764, Korea

(Received October 12, 2015 ; revised October 21, 2015 ; accepted October 28, 2015)

Abstract

To fabricate white LED having a high color rendering index value, red color phosphor mixed with the green color phosphor together in the blue chip, namely the blue chips with RG phosphors packaging is most favorable for high power white LEDs. In our previous papers, we reported on successful syntheses of $\text{Sr}_2\text{Si}_5\text{N}_8:\text{Eu}^{2+}$ and CaAlSiN_3 phosphors for red phosphor. In this work, for high power green phosphor, green-emitting ternary nitride $\text{Ba}_3\text{Si}_6\text{O}_{12}\text{N}_2:\text{Eu}^{2+}$ phosphor was synthesized in a high frequency induction furnace under N_2 gas atmosphere at temperatures up to 1400°C using EuF_3 as a raw material for Eu^{2+} dopant. The effects of molar ratio of component and experimental conditions on luminescence property of prepared phosphors have been investigated. The structure and luminescence properties of prepared $\text{Ba}_3\text{Si}_6\text{O}_{12}\text{N}_2:\text{Eu}^{2+}$ phosphors were investigated by XRD and photoluminescence spectroscopy. The excitation spectra of $\text{Ba}_3\text{Si}_6\text{O}_{12}\text{N}_2:\text{Eu}^{2+}$ phosphors indicated broad excitation wavelength range of 250 - 500 nm, namely from UV to blue region with distinct enhanced emission spectrum peaking at ≈ 530 nm.

Keywords : Oxonitridosilicate phosphor, White LED, $\text{Ba}_3\text{Si}_6\text{O}_{12}\text{N}_2:\text{Eu}^{2+}$, Photoluminescence

1. Introduction

LED is not a new invention and most of us are used to LEDs being red or green signal markers on Hi-Fi or television set. But these are so called low power LEDs. During the last couple of years high power LEDs, i.e. LEDs operating at powers of around 2 ~ 100 W, have reached a level of cost and performance that make them attractive to the general lighting industry. However, white LED which is essential to lighting industry has a still low color rendering index (CRI) problem for high light source efficiency (>180 lumen/watt) because energy-efficient LEDs often sacrifice color quality for efficiency. While many LEDs on the market today focus on maximum efficiency, objects illuminated by them can

appear unsaturated, washed out, or just outright strange. To increase color rendering index value, red color mixed with the green color of the adapted phosphors separately in the blue chip, namely the blue chips with RG phosphors packaging is most favorable for high light source efficiency of white LEDs. In our previous papers, we reported successful syntheses results of $\text{Sr}_2\text{Si}_5\text{N}_8:\text{Eu}^{2+}$ and $\text{CaAlSiN}_3:\text{Eu}^{2+}$ as a promising red phosphors¹⁻⁷⁾. In this work, for high light source efficiency of green phosphor, green-emitting ternary nitride $\text{Ba}_3\text{Si}_6\text{O}_{12}\text{N}_2:\text{Eu}^{2+}$ phosphor was synthesized in a high frequency induction furnace under N_2 gas atmosphere at temperatures up to 1400°C by using solid state second-step heat treatment process. SiN_4 -base covalent nitride materials, including nitridosilicates, nitridoaluminosilicates and $\text{CaAlSiN}_3:\text{Eu}^{2+}$ etc. are good host lattices for high power red phosphors. $\text{Ba}_3\text{Si}_6\text{O}_{12}\text{N}_2:\text{Eu}^{2+}$ is a layer-like oxonitridosilicate green phosphor and consists of vertex-sharing SiO_3N -tetrahedra forming as fundamental

*Corresponding Author : Hong-Ro Lee

Department of Advanced Materials Engineering, Chungnam National University
E-mail : leehr@cnu.ac.kr

building units. These nitride materials have strong absorption of the light emitted by the LED chips, i.e. UV (350 - 410 nm) or blue (440 - 480 nm) light. In general, the stronger absorption, the higher emitting efficiency. Another strong point is higher quantum or conversion efficiency. The other good point is chemical stability which refers to the stability in chemical composition and crystal structure of phosphor. Low chemical stability of a phosphor will not only make the production process more complex and costly, but also reduce the luminous efficiency and seriously shorten the lifetime of LED products. From these point of view, in this work, we focused on the synthesis of Eu^{2+} activated $\text{Ba}_3\text{Si}_6\text{O}_{12}\text{N}_2$ phosphors by the solid-state reaction method using multi-step heat treatment. Additionally these properties were compared with recently reported other reports on properties of phosphor synthesized from the ammonia nitridation of an oxide precursor in aqueous-solution. The excitation spectra of $\text{Ba}_3\text{Si}_6\text{O}_{12}\text{N}_2:\text{Eu}^{2+}$ phosphors indicated broad excitation wavelength range of 250 - 500 nm, namely from UV to blue region with distinct enhanced emission spectrum peaking at ≈ 530 nm. With an increase of Eu^{2+} ion concentration, the peak position of emission in spectra was red-shifted from 520 to 540 nm. Through multi-step heat treatment process, prepared phosphor showed excellent luminescence properties, such as high emission intensity and low thermal quenching. EuF_3 was used as a raw material for Eu^{2+} dopant with N_2 gas flowing instead of using commercial EuN chemical for $\text{Ba}_3\text{Si}_6\text{O}_{12}\text{N}_2:\text{Eu}^{2+}$ synthesis. In this work, we report on Eu^{2+} activated $\text{Ba}_3\text{Si}_6\text{O}_{12}\text{N}_2$ oxonitridosilicate green phosphor for white LEDs synthesized by solid state reaction

method using the second-step heat treatment. We have discussed the effect of the synthesis method on the relative emission characteristics by using photoluminescence (PL) and investigated the crystal structure by using powder X-ray diffraction (XRD).

2. Experimental

2.1 Synthesizing equipment and prepared chemicals

Raw material compositions for $\text{Ba}_3\text{Si}_6\text{O}_{12}\text{N}_2:\text{Eu}^{2+}$ synthesis are indicated in the Table 1. Synthesis process for phosphors by high frequency induction heating was shown in Fig. 1. The high frequency induction furnace have temperature range from R.T. to 2000°C and temperature rate with $100^\circ\text{C}/\text{min}$ (increase) and $300^\circ\text{C}/\text{min}$ (decrease) respectively. Vacuum was controlled as 10^{-3} Torr with 1000 ml/min N_2 gas flow rate.

2.2 Synthesis procedure and analysis

2.2.1 Synthesis of $\text{Ba}_3\text{Si}_6\text{O}_{12}\text{N}_2:\text{Eu}^{2+}$ phosphors

$\text{Ba}_3\text{Si}_6\text{O}_{12}\text{N}_2:\text{Eu}^{2+}$ phosphors were synthesized by using a multi-step heating process from raw materials mixtures of barium carbonate (BaCO_3 , 99.98%), silicon

Table 1. Prepared chemicals for $\text{Ba}_3\text{Si}_6\text{O}_{12}\text{N}_2:\text{Eu}^{2+}$ synthesis

Chemical	Molecular Formula	Purity (%)
Barium carbonate	BaCO_3	99.98
Silicon dioxide (Nano Powder)	SiO_2	99.50
Silicon nitride	Si_3N_4	99.90
Europium (III) fluoride	EuF_3	99.99
Activated carbon	C	99.00

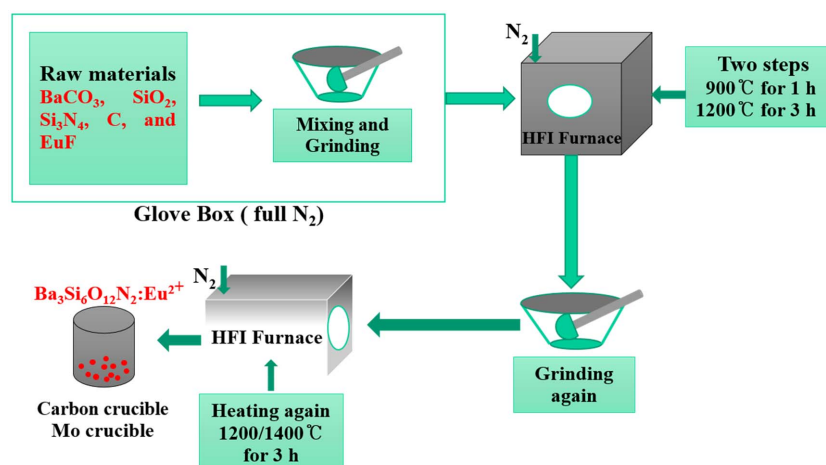
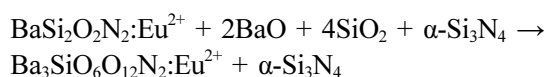


Fig. 1. Synthesis process for phosphors by high frequency induction heating.

dioxide (SiO_2 , 99.50%), europium (III) fluoride (EuF_3 , 99.99%), activated charcoal nano powder (C, 99.99%) and an excess of α -silicon nitride (α - Si_3N_4 , 99.90%). The concentration of Eu^{2+} varied in a range of 0 - 10 at% with respect to an excess of α -silicon nitride. They were stoichiometrically weighed and mixed thoroughly in an agate mortar. Mixtures were charged into a graphite crucible inside a glovebox under Ar atmosphere and placed in a radio-frequency (RF) induction furnace at maximum temperatures of 2000°C under N_2 atmosphere with a flow rate of 1000 ml/min during the heating process. For the first heating step, temperature was rapidly raised to 900°C and maintained for 1 h to decompose BaCO_3 completely. After then, temperature was increased to 1200°C and maintained for 3 h to form $\text{Ba}_3\text{Si}_6\text{O}_{12}\text{N}_2:\text{Eu}^{2+}$ phosphor, which is called 1st heat treated specimen. Finally, the 1st heat treated specimens were transferred into a molybdenum crucible to obtain more homogeneous powder product of highly crystalline state, and sintered again at 1200°C and 1400°C respectively under N_2 gas flow for 3 h to synthesize remaining small impurities of different Ba oxosilicate, $\text{BaSi}_2\text{O}_2\text{N}_2:\text{Eu}^{2+}$ to re-synthesize as $\text{Ba}_3\text{Si}_6\text{O}_{12}\text{N}_2:\text{Eu}^{2+}$ according to the reaction below⁸⁾;



After firing, the obtained 2nd heat treated phosphors were cooled down to 650°C with a rate of about $0.33^\circ\text{C}/\text{min}$ to offer best conditions for good crystallinity in a furnace under a continuous flow of N_2 gas. The atomic ratio Ba:Si:O:N = 3:6:12:2 of $\text{Ba}_3\text{Si}_6\text{O}_{12}\text{N}_2$ was confirmed by EDX (Energy-Dispersive X-ray Spectroscopy) analysis (Fig. 2).

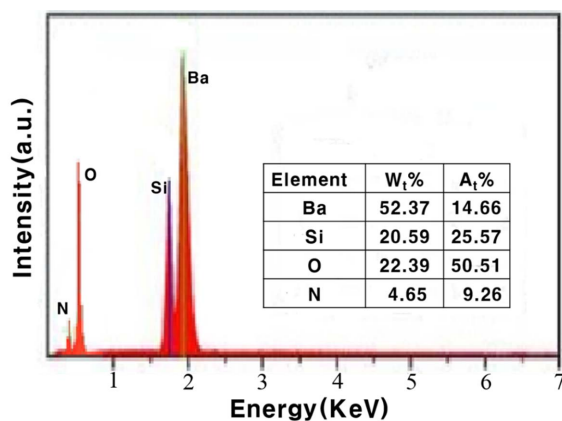


Fig. 2. EDX spectrum of 2nd heat treated $\text{Ba}_3\text{Si}_6\text{O}_{12}\text{N}_2:\text{Eu}^{2+}$ phosphor.

2.2.2 Structure and photoluminescence of $\text{Ba}_3\text{Si}_6\text{O}_{12}\text{N}_2:\text{Eu}^{2+}$

The crystalline structure of $\text{Ba}_3\text{Si}_6\text{O}_{12}\text{N}_2:\text{Eu}^{2+}$ powder was measured using X-ray powder diffraction (SIEMENS X-ray diffractometer) with Cu K_α radiation ($\lambda = 1.5406 \text{ \AA}$). The data were collected in the 2θ range from 10 to 70° with a scanning rate of $3^\circ/\text{min}$. Diffuse reflection spectra were obtained using a BaSO_4 powder calibrated UV-Vis spectrophotometer (UV-2200, SHIMADZU). Photoluminescence (PL) measurement was carried out at room temperature using 405 nm as the excitation wavelength with a Perkin Elmer LS-45 luminescence spectrometer. The temperature dependence of photoluminescence was measured with a multichannel spectrophotometer (model MCPD7000; Otsuka Electronics) equipped with temperature-controlled sample holders and a Xe lamp. Oxygen, nitrogen, and carbon residual impurity content of obtained phosphors were measured by using an oxygen/nitrogen analyzer (EMGA-930; HORIBA) and carbon/sulfur analyzer (SLE-CS-8520; SPECTRO).

3. Results and Discussion

3.1 Structure and residual concentration

Figure 3 gives the X-ray diffraction pattern of the 1st and 2nd heat treated specimen at 1200°C and 1400°C respectively for comparison. Most of the diffraction peaks of synthesized $\text{Ba}_3\text{Si}_6\text{O}_{12}\text{N}_2:\text{Eu}^{2+}$ phosphors showed identical peaks to the standard specimen and no apparent impurity phases were found. Moreover, it was also indicated that the doped

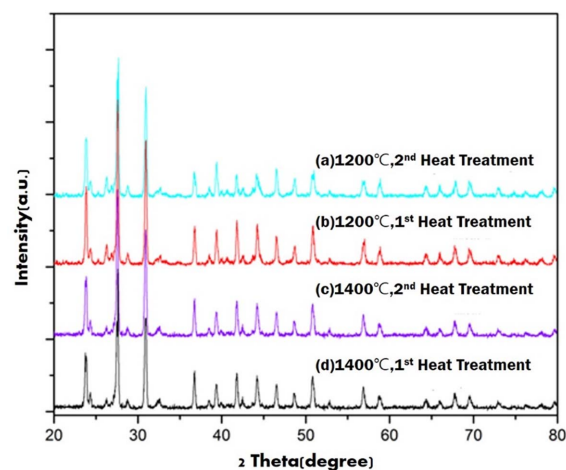


Fig. 3. XRD patterns of synthesized $\text{Ba}_3\text{Si}_6\text{O}_{12}\text{N}_2:\text{Eu}^{2+}$ phosphors (a) 1200°C , 2nd, (b) 1200°C , 1st, (c) 1400°C , 2nd and (d) 1400°C , 1st heat treatment.

Table 2. Oxygen, nitrogen, and carbon residual contents (wt%)

Ba ₃ Si ₆ O ₁₂ N ₂ :Eu ²⁺	O	N	C
1 st heat treated sample	36.56	3.65	0.08
2 nd heat treated sample	37.72	3.69	0.01
Ideal	38.09	3.70	0.00

Eu²⁺ ions did not caused any significant change in the host structure, because of close ionic radii of Ba²⁺, Si²⁺ and Eu²⁺. Activated carbon nano powder which was used as reductant to decompose oxide raw materials was also not detected. After the 1st heat treatment finishing, specimens were heat treated again each at 1200°C and 1400°C respectively to eliminate residual impurities as low as possible (Table 2). The crystal structure of obtained Ba₃Si₆O₁₂N₂:Eu²⁺ phosphors showed an trigonal crystal structure with lattice space group of P $\bar{3}$ (No.147) and lattice parameters of a=7.5046 Å and c=6.4703 Å⁸⁾.

3.2 Photoluminescence properties of Ba₃Si₆O₁₂N₂:Eu²⁺

In this work under near UV to blue light excitation a saturated green emission band with a peak wavelength of \approx 530 nm was observed. The broad excitation band enables efficient excitation at wavelengths below 450 nm. Fig. 4. shows emission band peak at \approx 530 nm of the Ba₃Si₆O₁₂N₂:Eu²⁺ (2 at %) phosphor at the excitation of 405 nm. Photoluminescence (excitation/emission) spectra of the Ba₃Si₆O₁₂N₂:Eu²⁺ (2 at %) phosphor exhibits an intense green body color due to absorption of Eu²⁺ in the blue

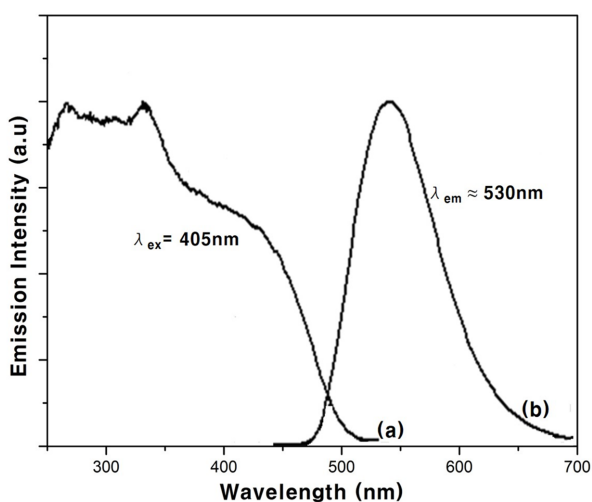


Fig. 4. Typical photoluminescence spectra of excitation (a) and emission. (b) of 1200°C, 2nd heat treated Ba₃Si₆O₁₂N₂:Eu²⁺ (2 at%) samples.

to green spectral range. Due to the high covalent environment around Eu²⁺ ion, emission of Ba₃Si₆O₁₂N₂:Eu²⁺ phosphors synthesized at 1200°C (Fig. 5(a), (b)) showed a fairly high intensity value but synthesized at 1400°C showed a little decreased intensity, which may be owing to mainly a decomposition of Ba₃Si₆O₁₂N₂ into BaSi₄O₆N₂ or to sintering behavior of this material⁸⁻⁹⁾. Through multi-steps heat treatment process residual impurities could be lowered as low as possible (Table 2), which result in fairly enhanced luminescence intensity.

3.3 Reflection spectra and emission intensity

The optical reflection spectra of Ba₃Si₆O₁₂N₂:Eu²⁺ phosphors with different Eu²⁺ ion concentration are shown in Fig. 6 (I, II, III). Reflection means total number of photons reflected and not absorbed by the

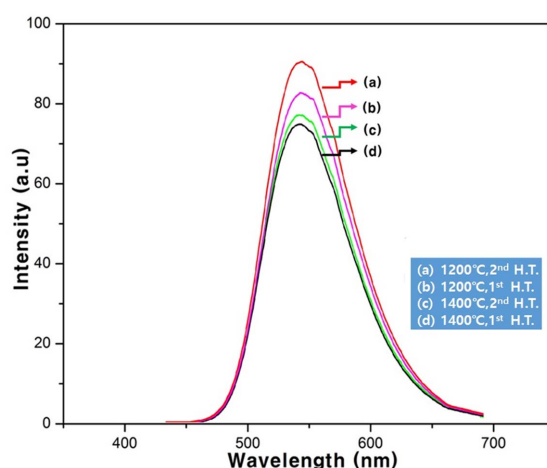


Fig. 5. Typical photoluminescence spectra of Ba₃Si₆O₁₂N₂:Eu²⁺ (2 at%) samples. (a) 1200°C, 2nd, (b) 1200°C, 1st, (c) 1400°C, 2nd and (d) 1400°C, 1st heat treatment.

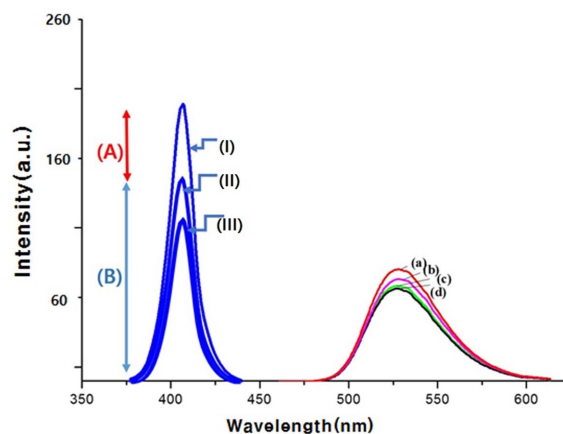


Fig. 6. Reflection spectra of (Ba_{3-x}Eu_x)Si₆O₁₂N₂ phosphor relation to emission intensity. (a) 2.0, (b) 4.0, (c) 6.0 and (d) 1.0 at % of Eu²⁺.

phosphor. According to reflection light curves (II, III) become decreased comparing to excited light curve (I), namely absorption part (A) increase relatively to reflection part (B), the efficiency of the phosphor performance in absorbing an external excitation light increase. This high absorbing efficiency as well as consistency are required for high quantum efficiency of phosphor. The absorption is related to the electronic transition of the $\text{Ba}_3\text{Si}_6\text{O}_{12}\text{N}_2$ host and the $4f^7(^8S_{7/2}) \rightarrow 4f^65d^1$ transition of Eu^{2+} ion⁸⁾. When applying excited light (curve (I)), as the reflection intensity changed from curve (II) to curve (III), absorption intensity (A) was increased and reflection intensity (B) was decreased. This may be caused by strong absorption according to increasing Eu^{2+} concentration up to 2 at% (i.e. $x = 0.02$), which means to become gradually distinct green-emitting state. At 2 at% Eu^{2+} concentration, $\text{Ba}_3\text{Si}_6\text{O}_{12}\text{N}_2:\text{Eu}^{2+}$ phosphors showed lowest reflection intensity (III) but highest emission intensity (Fig. 4 curve (a)).

Dependence of emission intensity and peak emission wavelength on Eu^{2+} concentration of the $(\text{Ba}_{3-x}\text{Eu}_x)\text{Si}_6\text{O}_{12}\text{N}_2$ phosphor is shown in Fig. 7. With increasing Eu^{2+} content, emission intensity of $(\text{Ba}_{3-x}\text{Eu}_x)\text{Si}_6\text{O}_{12}\text{N}_2$ phosphor was maximized at a Eu^{2+} concentration of around 2 at% (i.e. $x = 0.02$) and then decreased slowly with more Eu^{2+} doping. The decrease in emission intensity concentration quenching which is mainly caused by the energy transfer between two Eu^{2+} ions^{8,10)}. Meanwhile, the peak emission of $(\text{Ba}_{3-x}\text{Eu}_x)\text{Si}_6\text{O}_{12}\text{N}_2$ phosphor shifted to the longer wavelength side (red shift) as Eu^{2+} concentration increased from 0 to 6 at%. The highest PL

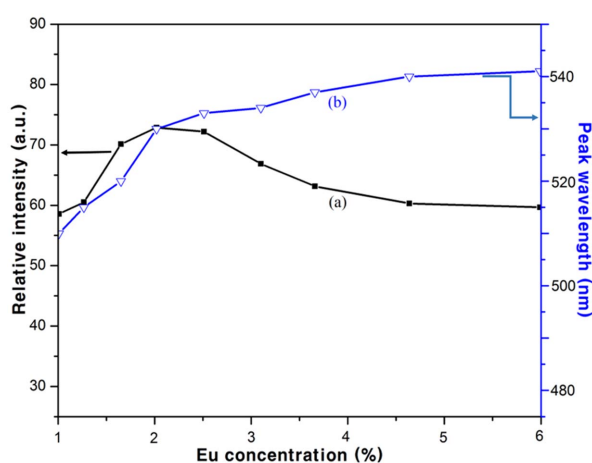


Fig. 7. Dependence of emission intensity (a) and emission peak wavelength (b) as a function of Eu concentration in $(\text{Ba}_{3-x}\text{Eu}_x)\text{Si}_6\text{O}_{12}\text{N}_2$ phosphor under 405 nm excitation.

intensity was found at $x = 0.02$ and further increase of Eu doping concentration lead to obvious decrease of emission intensity. The intensity decrease above $x = 0.02$ can be attributed to the concentration quenching, which may be caused by the non-radiative energy transfer between active ions or between active ion and host^{8,11)}.

3.4 Emission intensity according to time period during 2nd heat treatment

Effect of heat treatment period during 2nd heating process on emission intensity of $\text{Ba}_3\text{Si}_6\text{O}_{12}\text{N}_2:\text{Eu}^{2+}$ (2 at %) phosphor was shown in Fig. 8. The highest emission intensity was observed at the 3 h heat treatment duration time. This means that 3h heat treatment is adequate to substitute Ba atoms with Eu^{2+} to reveal efficient emission intensity because the bonding of the Ba atoms is highly ionic with only the $4p^{3/2}$ participating in covalent bonds⁸⁾. However when holding time was increased beyond 3 h treatment, emission intensity showed an obvious decreasing tendency. This may be caused by thermal ionization of the overexcited 5d electron of Eu^{2+} ¹⁰⁾.

Effect of heat treatment temperature during 2nd process on luminescence intensity of $\text{Ba}_3\text{Si}_6\text{O}_{12}\text{N}_2:\text{Eu}^{2+}$ was shown in Fig. 9. With heat treatment temperature increasing, the emission intensity of $\text{Ba}_3\text{Si}_6\text{O}_{12}\text{N}_2:\text{Eu}^{2+}$ increased and showed maximum value at 1200°C. But with increasing temperature over 1200°C, emission intensity was decreased obviously. This result can be explained a few decomposition of $\text{Ba}_3\text{Si}_6\text{O}_{12}\text{N}_2$ mainly into $\text{BaSi}_4\text{O}_6\text{N}_2$ or some sintering behavior of this material at high temperature¹¹⁾.

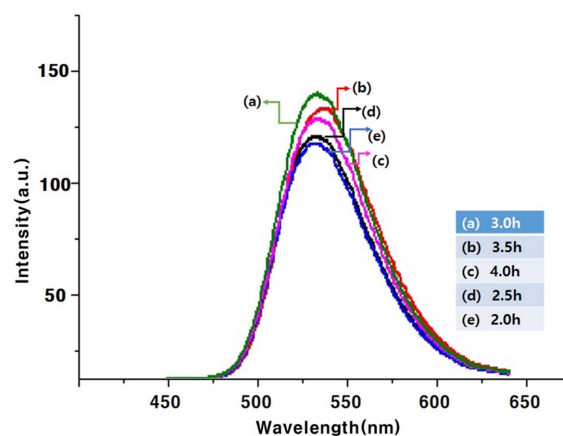


Fig. 8. Emission intensity of $\text{Ba}_3\text{Si}_6\text{O}_{12}\text{N}_2:\text{Eu}^{2+}$ (2 at %) according to heat treatment period. (a) 3.0 h, (b) 3.5 h, (c) 4.0 h, (d) 2.5 h and (e) 2.0 h.

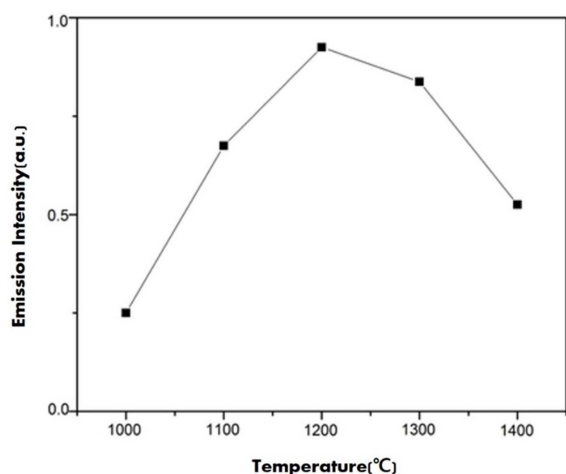


Fig. 9. Emission intensity of $\text{Ba}_3\text{Si}_6\text{O}_{12}\text{N}_2:\text{Eu}^{2+}$ (2 at%) according to synthesis temperature.

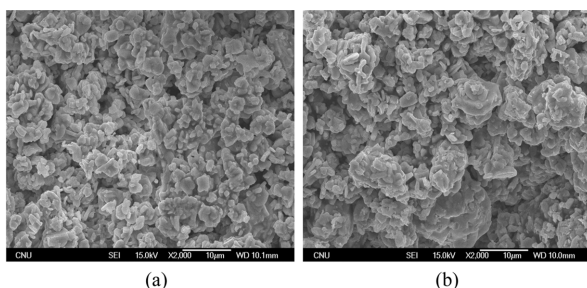


Fig. 10. SEM micrographs according to temperature during 2nd heat treatment process. (a) 1200°C and (b) 1400°C.

Figure 10 shows an SEM photograph of the Eu^{2+} activated $\text{Ba}_3\text{Si}_6\text{O}_{12}\text{N}_2$ phosphors, which were synthesized at 1200°C for 3h (a) and 1400°C for 3h (b). Comparing images (a) with (b), heat treatment at 1200°C enhances the crystallization of the host lattice and decreases surface defects. This indicates that the $\text{Ba}_3\text{Si}_6\text{O}_{12}\text{N}_2:\text{Eu}^{2+}$ phosphor synthesized at 1200°C has a good dispersion and a regular shape of crystal than phosphors synthesized at 1400°C. Fig. 11 shows particle size distribution measured by Mastersizer

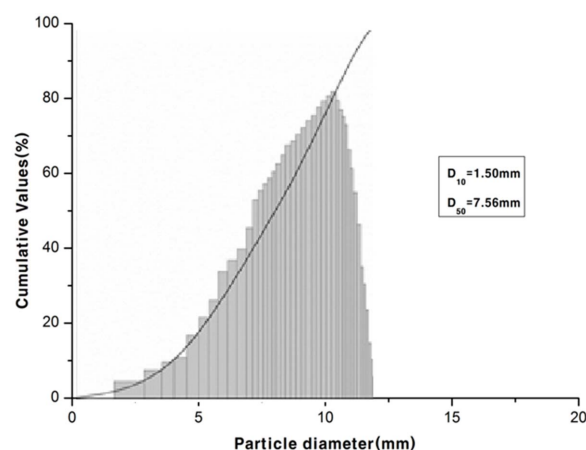


Fig. 11. Particle size distribution of phosphors obtained after 2nd heat treatment process.

3000E particle analyzer. Particle sizes of the synthesized powders were about 6~12 μm .

Figure 12(a) shows $\text{Ba}_3\text{Si}_6\text{O}_{12}\text{N}_2:\text{Eu}^{2+}$ phosphors of the as-prepared according to Eu^{2+} concentration. The highest emission (circled) was observed at 2 at% concentration. Fig. 12(b) shows $\text{Ba}_3\text{Si}_6\text{O}_{12}\text{N}_2:\text{Eu}^{2+}$ phosphors obtained according to synthesis temperature. Distinguished enhanced luminescence (circled) was observed at 1200°C synthesis but others rather showed a little decreased intensity.

3.5 T. Temperature quenching of $\text{Ba}_3\text{Si}_6\text{O}_{12}\text{N}_2:\text{Eu}^{2+}$

Phosphors for white LED should have low thermal quenching to avoid changes in chromaticity and brightness of white LED at high temperatures. The temperature-dependent emission intensity of $\text{Ba}_3\text{Si}_6\text{O}_{12}\text{N}_2:\text{Eu}^{2+}$ (2 at. %) phosphors according to synthesis conditions are shown in Fig. 13. As the temperature increased from 20 to 200°C, emission intensity of $\text{Ba}_3\text{Si}_6\text{O}_{12}\text{N}_2:\text{Eu}^{2+}$ phosphor obtained from solid-state 2nd heat treatment synthesis maintained relatively stable value comparing to 1st heat treatment phosphor

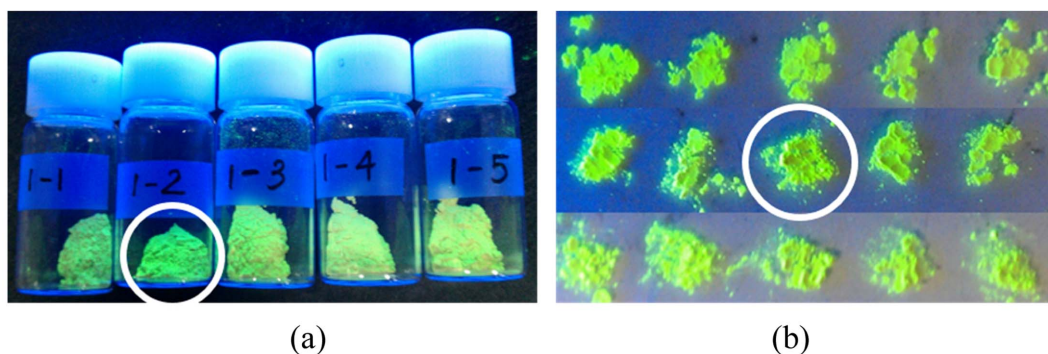


Fig. 12. Emission comparison according to Eu^{2+} concentration: 1, 2, 3, 4, 5 at% from left to right (a) and synthesis temperature 1200°C (circled) with 2 at% Eu^{2+} (b)

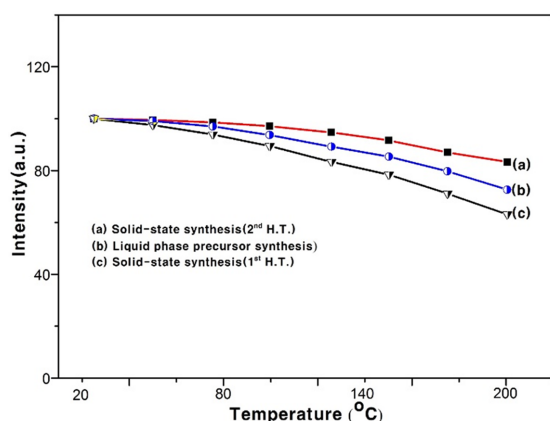


Fig. 13. Temperature quenching of $\text{Ba}_3\text{Si}_6\text{O}_{12}\text{N}_2:\text{Eu}^{2+}$ phosphor synthesized at 1200°C . (a) Solid-state synthesis, 2nd heat treated, (b) Liquid phase precursor synthesis, and (c) Solid-state synthesis, 1st heat treated.

and also higher value than reported value of liquid phase precursor synthesized phosphor¹²⁻¹³. A high and a more consistent quantum efficiency, which is related to temperature quenching is desirable for valuable phosphor performance.

4. Conclusion

Green-emitting $\text{Ba}_3\text{Si}_6\text{O}_{12}\text{N}_2:\text{Eu}^{2+}$ phosphor was successfully prepared by multi-step high frequency induction heat treatment method. XRD analysis showed the single-phase crystal structure of $\text{Ba}_3\text{Si}_6\text{O}_{12}\text{N}_2$. The excitation spectra of $\text{Ba}_3\text{Si}_6\text{O}_{12}\text{N}_2:\text{Eu}^{2+}$ phosphors showed broad excitation wavelength range of 250 - 500 nm with distinct enhanced emission peaks, which means this phosphor is suitable for application of white LED with UV or blue chip. With an increase of Eu^{2+} ion concentration, the peak position of emission in spectra was red-shifted from 520 to 540 nm. At 2 at% concentration of Eu^{2+} ions in synthesized phosphor, maximum green emission peak at ≈ 530 nm was obtained under 405nm blue light excitation. The emission peak intensity of $\text{Ba}_3\text{Si}_6\text{O}_{12}\text{N}_2:\text{Eu}^{2+}$ phosphors obtained from solid-state 2nd heat treatment synthesis maintained relatively

stable value compared to 1st heat treatment phosphor and also higher value than reported value of liquid phase precursor synthesized phosphor. $\text{Ba}_3\text{Si}_6\text{O}_{12}\text{N}_2:\text{Eu}^{2+}$ phosphors synthesized at 1200°C showed most efficient emission peak but at 1400°C , decreased partly due to sintering behavior of this phosphor and thermal ionization of Eu^{2+} .

Acknowledgement

This study was financially supported by research fund of Chungnam National University in 2014.

References

1. Wen Tao Zhang, Hong-Ro Lee, J. Korea. Inst. Surf. Eng., 40 (2007) 235.
2. Wen Tao Zhang, Hong-Ro Lee, Applied Optics, 49(2010) 2566.
3. Wen Tao Zhang, Hong-Ro Lee, Phosphorus, Sulfur, and Silicon and the Related Elements, 185 (2010) 134.
4. Van Duong Luong, Wen Tao Zhang and Hong-Ro Lee, J. of Alloys and Compound, 509 (2011) 7525.
5. Wen Tao Zhang, Hong-Ro Lee, J. of Photochemistry and Photobiology A:Chemistry, 218 (2011) 1.
6. Van Duong Luong, Wen Tao Zhang and Hong-Ro Lee, Advanced Materials Research, 233 (2011) 2705.
7. Van Duong Luong, Hong-Ro Lee, J. Korea. Inst. Surf. Eng., 47 (2014) 192.
8. Cordula Braun, Markus Seibald, Oliver Oeckler, and Wolfgang Schnick, OChem. Eur. J., pt. Express., 16 (2010) 9646.
9. Chenxia Li, Hong Chen, and Shiqing Xu, International Journal for Light and Electron Optics, 126 (2015) 499.
10. Yousuke Kotuska, Takeshi Fukuda, and Norihiko Kamata, Materials Letters, 145 (2015) 158.
11. Shilong Zhao, Hongping Ma, and Shiqing Xu, Optics Communications, 295 (2013) 129.
12. D. H. Yoon, K. Toda, T. Masaki and Y. H. Song et al., Mater. Letters 77 (2012) 121.
13. Eun-Hee Kang, Sung-Woo Choi, and Seong-Hyeon Hong, J. Solid State Sci. Techno, 1 (2012) R11.